Electrowetting retroreflectors: Scalable and wide-spectrum modulation between corner cube and scattering reflection

M. K. Kilaru, B. Cumby, and J. Heikenfeld[a)]
Department of Electrical and Computer Engineering, Novel Devices Laboratory, University of Cincinnati, Cincinnati, Ohio 45221, USA

(Received 26 September 2008; accepted 20 December 2008; published online 27 January 2009)

Corner cube and spherical retroreflectors are ubiquitous in conspicuity and range-finding applications since they reflect light back to the illumination source with unmatched efficiency. We report here a switchable electrowetting retroreflector platform that provides multiple novel features, including (a) using $<0.5\ \mu J/cm^2$ electrical energy to switch from a light scattering state, (b) low loss and wide spectrum as limited only by the absorption spectrum of water, (c) use of ultrasimple self-assembly of 10^3-10^5 liquid lenslets/in.^{2} on a polymer/Al corner-cube substrate, and (d) change in retroreflected irradiance of $>10:1$ over a $\pm 30°$ field of view. © *2009 American Institute of Physics*. [DOI: 10.1063/1.3073840]

Retroreflectors are most often comprised of glass beads or a truncated corner of a cube, with the latter exhibiting several fold higher retroreflective efficiency.[1,2] The reflected light emerges parallel to the direction of the incident ray. As a result, an observer positioned next to the illumination source perceives a surface that is 50 times brighter than a diffusely reflecting surface, such as paper. Retroreflectors are commercially found in sizes ranging from bulk optic scales (centimeters) to microreplicated polymer films with corner cubes that individually measure tens of microns.[3] Over the past decade, switchable retroreflectors[4,5] have been demonstrated for free-space communications. There has not been focus, however, on naked eye applications because (1) prior approaches such as microelectromechanics[4] are difficult to scale to the arrays sizes needed for visualization at a distance and (2) prior approaches such as multiple-quantum wells[5] are typically limited to very narrow-spectrum infrared. Therefore, scalability and wide spectrum must be realized before naked eye applications can be pursued (e.g., consider the requirements for conventional retroreflective traffic safety signs). Reported herein are first results on electrowetting[6] retroreflectors that are far faster than the response of the human eye, are arguably scalable to large dimensions, and which exhibit wide-spectrum modulation between retroreflection and scattering reflection. These results could prove useful for a variety of applications including, but not limited to, flashing safety markings (personal, road, or structural), surveying and range finding, free-space communications, active decorative films, and military friend-foe ID.

The electrowetting retroreflector device structure is shown in Fig. 1 and is fabricated as follows. Arrayed corner cubes of $\sim 800\ \mu m$ individual size were microreplicated in a polymer substrate. The corner-cube array was then coated with a reflective electrode and a hydrophobic dielectric. Next, oil/water is self-assembled into the corner cubes via dip coating through an oil film floating on water.[7] The device is then top sealed with glass coated with a transparent conductor. The total active area of the device tested herein was $\sim 10\ cm^2$. Further fabrication details are available in the supplementary online document for this manuscript.[8] The demonstrated fabrication process is highly scalable and is comparatively simple with respect to the prior art.[4,5] Also, unlike some forms of optofluidic devices,[9,10] the retroreflector device is self-contained and requires no special peripherals, such as syringe pumps. Once assembled, the electrowetting retroreflector in the zero-voltage stage exhibits a scattering reflection. As shown in Fig. 1(b), the meniscus between the low index water and higher index oil forms a concave lenslet[11] that breaks up the optical symmetry of the corner cube. The concavity of the lens is determined by Young's contact angle for the water on the hydrophobic surface ($\theta_Y > 160°$). The materials implemented herein well ex-

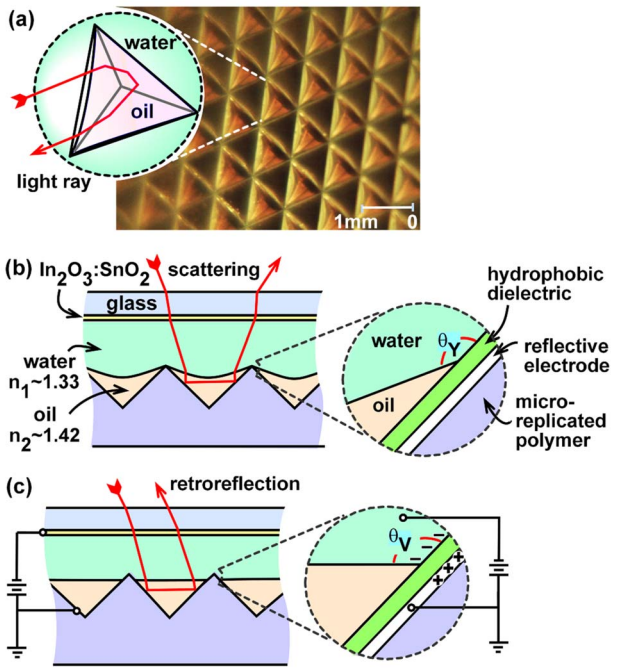


FIG. 1. (Color online) Arrayed electrowetting corner cube retroreflectors. (a) Photograph of an array of corner cubes dosed with red oil and covered with water. (b) Diagram with no applied voltage and an oil/water meniscus that forms a light scattering lenslet. (c) Electrowetting the oil/water meniscus to a flat geometry and thereby exhibiting retroreflection.

[a)]Tel.: 513-556-4763. Electronic addresses: heikenjc@email.uc.edu and jason.c.heikenfeld@uc.edu.

 © 2009 American Institute of Physics

Downloaded 15 May 2009 to 129.137.202.77. Redistribution subject to AIP license or copyright; see http://apl.aip.org/apl/copyright.jsp

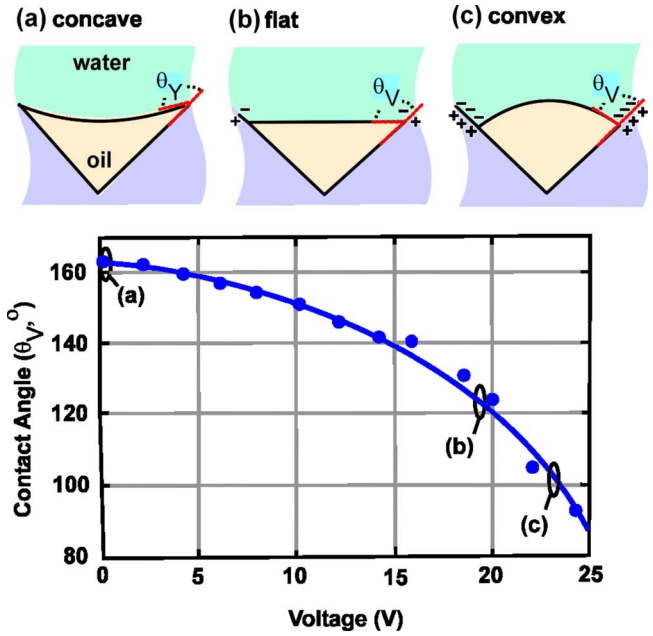


FIG. 2. (Color online) Plot of the electrowetted contact angle (θ_V) vs voltage and diagrams of relation to lenslet geometry inside each corner cube.

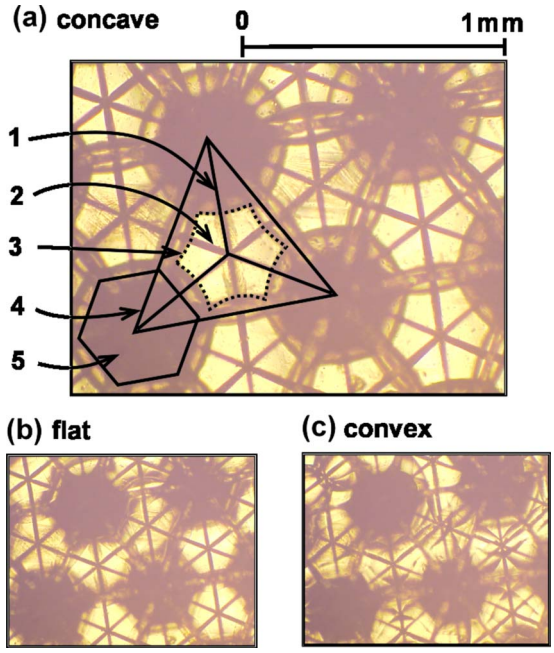


FIG. 3. (Color online) Topside illuminated microscope photographs of electrowetting retroreflectors: (a) 0 V and concave lenslet, (b) 19 V and a flat lenslet, and (c) 25 V and a convex lenslet.

ceed the minimum requirement for concavity ($\theta_Y \sim 125°$) as calculated from the corner cube's side-wall slope (180°–54.74°). To an observer of the electrowetting retroreflector in this zero-voltage state, the retroreflector appearance is optically scattering or semidiffuse.

Electrowetting[6] is utilized to activate the retroreflector by restoring the optical symmetry of the corner cube. As shown in Fig. 1(c), a voltage is applied between the water and the reflective electrodes beneath the hydrophobic dielectric. This induces charge accumulation, an electromechanical force,[12] and results in a reduced contact angle projection (θ_V).[13] This reduction in contact angle alters the radius of curvature of the oil/water meniscus similar to that recently reported for electrowetting microwells.[14] The response of contact angle θ_V to applied voltage is plotted in Fig. 2 and can be explained by the so-called electrowetting equation,[6]

$$\cos\,\theta_V = \cos\,\theta_Y + \frac{1}{2}\frac{\varepsilon V^2}{\gamma d}, \tag{1}$$

which includes the hydrophobic dielectric capacitance per unit area (ε/d, F/m^2), the applied dc voltage or ac rms voltage (V), the water/oil interfacial surface tension (γ, mN/m), and Young's contact angle at zero voltage (θ_Y, °). As shown in Fig. 2 with increasing voltage, the lenslet first transitions from concave to flat at 19 V. To an observer of the electrowetting retroreflector in this flat meniscus state, the retroreflector appearance is ten times brighter than all other surrounding surfaces. With additional voltage the meniscus then further transitions to convex and a light scattering state is again achieved. The electrowetting retroreflector reported herein utilizes the simplest embodiment of a low-capacitance Parylene/fluoropolymer dielectric. However, it has been recently shown that high capacitance dielectrics[14] would permit switching of the retroreflectors reported herein with <5 V. Regardless of the dielectrics chosen, given a γ of ~ 5 mN/m and assuming a planar surface the total energy consumption per modulation is calculated to be $<0.5\ \mu$J/m^2 (includes both $\frac{1}{2}CV^2$ resistance and capacitance). A more precise calculation would reveal even lower energy per modulation because the water is an electrode and only contacts a small fraction of the dielectric surface (Fig. 1).

Turning the attention to Fig. 3, photographs of the electrowetting retroreflector are taken through a microscope with top-side illumination. The dark lines shown in the photo represent the following: (1) corners of the cube, (2) reflection of the corner of cube off an opposing cube facet, (3) the oil/water/dielectric contact line, (4) the top ridge defining each triangular corner cube well, and (5) the area that does not support retroreflection.[1] The hexagonal shaped dark area that does not support retroreflection is typical of all corner cube retroreflectors and is not unique to the device described herein. Analyzing the photographs in Fig. 3 as a function of voltage, one can clearly see the straightening (flattening) of the oil/water/dielectric contact line in Fig. 3(b). A comment should also be made back to the photograph shown in Fig. 1(a). The photograph was taken with the light source and the camera at different angles such that the red oil could be imaged through reflection off only a subset of the corner-cube facets. Therefore one should not relate the photograph in Fig. 1(a) to retroreflective behavior.

An experimental measure of retroreflective behavior over $\pm 45°$ is shown in Fig. 4. A beam splitter was utilized to align along a single optical axis the retroreflector array, a beam-expanded 633 nm laser, and a photodiode positioned 40 cm from the retroreflector array (a diagram is available in the online supplementary materials[8]). The laser beam area was ~ 0.8 cm^2 and covered ~ 300 corner cubes. The measured contrast ratio between the detected irradiance at 19 V (flat meniscus) and at 0 V (concave meniscus) is at least 10:1 over a wide field of view of $\pm 30°$. This wide field of view is partially due to corner cubes that are filled with oil ($n \sim 1.42$), thereby causing refraction and an internal reduction in the incidence angle.[1,2] The presence of two "wings" in the angular profile at +20° and −20° is not well understood at this time.

Downloaded 15 May 2009 to 129.137.202.77. Redistribution subject to AIP license or copyright; see http://apl.aip.org/apl/copyright.jsp

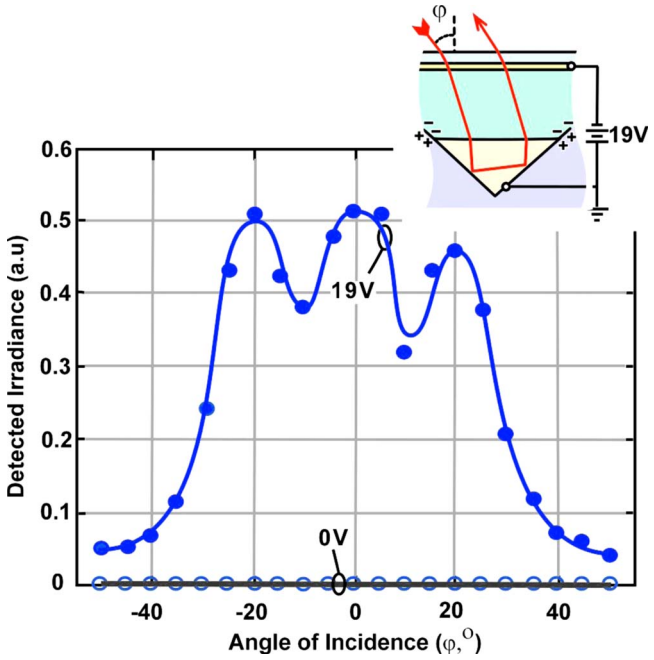


FIG. 4. (Color online) Retroreflected irradiance vs incident angle in the concave (0 V) and flat meniscus states (19 V) as measured for ~300 corner cubes covering an area of ~0.8 cm^2.

The results presented in Figs. 1–4 form the basis of discussion for other factors that should be considered for electrowetting retroreflectors. First, metal or dielectric reflectors and a grid-style electrode on the front glass would promote reflection spanning from the ultraviolet to the infrared. The operational spectrum is primarily limited by the vibrational spectrum of water in the infrared. However, in microscale corner cubes, the water layer is easily <100 μm thick. Therefore, the device would no longer be the limiting attenuator in typical atmospheric environments (i.e., humidity). In the absence of absorptive losses, the maximum retroreflective efficiency can be approximated as

$$I_R = I_0(1-F) \times R^3/\sqrt{3}, \quad (2)$$

where I_R and I_0 are the retroreflected and irradiated power densities, respectively, F is approximately the sum of Fresnel reflections for the optical layers of the device, R is the metal reflectivity, and the $3^{-1/2}$ factor arises from the maximum retroreflective area of the corner cubes (visually shown in Fig. 3). For the materials utilized herein, an antireflection coating on only the front glass surface, $F \sim 0.14$, and $R \sim 0.90$, the maximum I_R can be ~36%. Regarding the increased scattering and field of view, higher index oils, such as chloronapthalene ($n \sim 1.63$) were shown to electrowet, comparable to dodecane ($n \sim 1.42$). The low Abbe number of high index oils (dispersion) is not a concern because only retroreflecting and optically scattering states are desired. Switching speed should also be discussed. It is not possible for electrowetting retroreflectors to provide >1 MHz switching speeds associated with the multiple-quantum-well approach.[5] For the devices tested herein (~800 um, $\gamma \sim 5$ mN/m), switching with a contrast of >10:1 was demonstrated at a rate of ~200 Hz. Assuming corner cubes that measure ~10 μm on a side, 1 μm of water/oil contact line movement, and 10 cm/s contact line velocity ($\gamma \sim 50$ mN/m), a switching speed of 100 kHz is calculated.[15] Meniscus oscillation is not a concern because the electrowetting retroreflector requires only two contact angle states and therefore can be designed for critically damped switching.[11] It should be noted that scaled-down retroreflectors will eventually lead to substantial diffractive losses.[16] However, even a 10 μm sized corner cube is still ~20 times the size of visible light. Regarding beam divergence, the oil/water meniscus might not be perfectly flat as a result of contact angle hysteresis.[6] For example, ~1° of contact angle hysteresis will cause ~0.5° of additional beam divergence. Some beam divergence is actually beneficial for naked eye applications because the illuminating source and the eye are rarely collinear. Lastly, regarding reliability, devices were tested out to 120 000 operations without loss of contrast (>10:1), with more than millions of cycles expected based on the longevity of commercially available Varioptic electrowetting lens products.

The authors would like to thank S. Scott of Reflexite Inc. for providing corner-cube templates, and S. Haught of Army CERDEC for input and encouragement and primary financial support commencing in 2009. The authors acknowledge existing support of this work by an AFOSR Young Investigator Award No. 06NE223 and in part by a NSF CAREER Award No. 0640964.

[1] H. D. Eckhardt, Appl. Opt. **10**, 1559 (1971).
[2] V. A. Handerek and L. C. Laycock, Proc. SPIE **5614**, 1 (2004).
[3] http://www.reflexite.com/.
[4] D. S. Gunawan, L.-Y. Lin, and K. Pister, Sens. Actuators, A **47**, 580 (1995).
[5] W. S. Rabinovich, P. G. Goetz, R. Mahon, L. Swingen, J. Murphy, M. Ferraro, H. R. Burris, Jr., C. I. Moore, M. Suite, G. C. Gilbreath, and S. Binari, Opt. Eng. **46**, 10400 (2007).
[6] F. Mugele and J. C. Baret, J. Phys.: Condens. Matter **17**, R705 (2005).
[7] B. Sun, K. Zhou, Y. Lao, J. Heikenfeld, and W. Cheng, Appl. Phys. Lett. **91**, 011106 (2007).
[8] See EPAPS Document No. E-APPLAB-94-045904 for additional details on fabrication and characterization. For more information on EPAPS, see http://www.aip.org/pubservs/epaps.html.
[9] U. Levy and R. Shamai, Microfluid. Nanofluid. **4**, 97 (2008).
[10] D. Psaltis, S. R. Quake, and C. Yang, Nature (London) **442**, 381 (2006).
[11] S. Kuiper and B. H. W. Hendriks, Appl. Phys. Lett. **85**, 1128 (2004).
[12] T. B. Jones, J. Micromech. Microeng. **15**, 1184 (2005).
[13] F. Mugele and J. Buehrle, J. Phys.: Condens. Matter **19**, 375112 (2007).
[14] K. Zhou and J. Heikenfeld, Appl. Phys. Lett. **92**, 113515 (2008).
[15] N. R. Smith, L. Hou, J. Zhang, and J. Heikenfeld, Proceedings of the IEEE UGIM, 2008, p. 11, http://ieeexplore.ieee.org/stamp/stamp.jsp?arnumber=04573188.
[16] H. Ichikawa, J. Opt. A, Pure Appl. Opt. **6**, S121 (2004).

Downloaded 15 May 2009 to 129.137.202.77. Redistribution subject to AIP license or copyright; see http://apl.aip.org/apl/copyright.jsp